

# Thermal Properties of Extruded/Injection-Molded Poly(lactic acid) and Biobased Composites

Abdellatif A. Mohamed,<sup>1</sup> V. L. Finkenstadt,<sup>2</sup> D. E. Palmquist<sup>3</sup>

<sup>1</sup>Cereal Products & Food Science Unit, National Center for Agriculture Utilization Research, U.S. Department of Agriculture Agricultural Research Service, 1815 North University Drive, Peoria, Illinois 61604

<sup>2</sup>Plant Polymer Research Unit, National Center for Agriculture Utilization Research, U.S. Department of Agriculture Agricultural Research Service, 1815 North University Drive, Peoria, Illinois 61604

<sup>3</sup>Area Statistician; National Center for Agriculture Utilization Research, U.S. Department of Agriculture Agricultural Research Service, 1815 North University Drive, Peoria, Illinois 61604

Received 8 December 2006; accepted 23 February 2007

DOI 10.1002/app.26496

Published online 27 September 2007 in Wiley InterScience (www.interscience.wiley.com).

**ABSTRACT:** To determine the degree of compatibility between poly(lactic acid) and different biomaterials (fibers), poly(lactic acid) was compounded with sugar beet pulp and apple fibers. The fibers were added in 85 : 15 and 70 : 30 poly(lactic acid)/fiber ratios. The composites were blended by extrusion followed by injection molding. Differential scanning calorimetry and thermogravimetric analysis were used to analyze the extruded and extruded/injection-molded composites. After melting in sealed differential scanning calorimetry pans, the composites were cooled through immersion in liquid nitrogen and aged (stored) at room temperature for 0, 7, 15, and 30 days. After storage, the samples were heated from 25 to 180°C at 10°C/min. The neat poly(lactic acid) showed a glass-transition at 59°C with a change in heat capacity ( $\Delta C_p$ ) value of 0.464. The glass transition was followed by crystallization and melting transitions. The enthalpic relaxation of the poly(lactic acid) and composites steadily increased as a function of the storage time. Although the presence of fibers had little effect on the enthalpic relaxation, injection molding reduced the enthalpic relaxation. The crystallinity percentage of the unprocessed neat poly(lactic acid) dropped by 95% after extrusion and by 80% for the extruded/injection-molded composites. The degradation

was performed in air and nitrogen environments. The degradation activation energy of neat poly(lactic acid) exhibited a significant drop in the nitrogen environment, although it increased in air. This meant that the poly(lactic acid) was more resistant to degradation in the presence of oxygen. Overall, injection molding appeared to reduce the activation energy for all the composites. Sugar beet pulp significantly reduced the activation energy in a nitrogen environment. In an air environment, both sugar beet pulp and apple fibers increased the activation energy. The enzymatic degradation of the composites showed a higher degradation rate for the extruded samples versus the extruded/injection-molded composites, whereas the apple composites exhibited higher weight loss. The thermogravimetric analysis data showed that the degradation of unprocessed and extruded neat poly(lactic acid) followed a one-step mechanism, whereas extruded/injection-molded composites showed two-step degradation. A higher fiber content resulted in up to three-step degradation mechanisms. © 2007 Wiley Periodicals, Inc. *J Appl Polym Sci* 107: 898–908, 2008

**Key words:** ageing; biodegradable; differential scanning calorimetry (DSC); thermal properties; thermogravimetric analysis (TGA)

## INTRODUCTION

Despite the convenience and practicality of petroleum-based polymers for food and other consumer-good packaging, there is evidence for ecological dis-

turbance. The development and use of biodegradable plastics in packaging for environmental protection have been stimulated by public concerns and interest. Polymer composites are usually prepared from materials with dissimilar properties. Most polymer composites are difficult to recycle, or substantial costs are incurred for disposal. Green composites use agriculturally based polymers and biodegradable plant-based fillers.<sup>1</sup> Poly(lactic acid) (PLA) is a hydrophobic polymer prepared from agricultural byproducts with lactic acid fermentation followed by polymerization. PLA is biodegradable, possesses properties comparable to those of petroleum-based polymers, and can be extruded (EX) and injection-molded, but it is more expensive.<sup>2,3</sup> PLA degradation products in soil or water are not toxic to the environment. Apples represent a major fruit

Names are necessary to report factually on available data; however, the U.S. Department of Agriculture neither guarantees nor warrants the standard of the product, and the use of the name by the U.S. Department of Agriculture implies no approval of the product to the exclusion of others that may also be suitable.

Correspondence to: A. A. Mohamed (a.mohamed@ars.usda.gov).

*Journal of Applied Polymer Science*, Vol. 107, 898–908 (2008)  
© 2007 Wiley Periodicals, Inc. \*This article is a US Government work and as such is in the public domain in the United States of America.

commodity throughout the year in the United States because of the market availability, diversity of cultivars, and variety of products, such as fresh fruit, juice, and cider. Sugar beets (15% sugar; *Beta vulgaris*) are grown as a commercial crop in many countries such as France, Germany, Turkey, Russia, Poland, the Ukraine, and the United States. As the source of about one-third of the world supply of sugar, sugar beets are an important agricultural commodity. The U.S. sugar beet industry is estimated to be \$1.27 billion annually, and over 400 million metric tons of wet pulp is generated each year. Sugar beet pulp (SBP) is usually used as a low-value animal feed or is disposed of at an additional cost. The future profitability of the beet sugar processing industry will depend on the development of new ways to use this byproduct. PLA has been blended with fibers,<sup>4-6</sup> polymers,<sup>7-11</sup> and inorganic fillers.<sup>12,13</sup> PLA/SBP composites have been investigated before; however, because of dissimilar preparation methods, it is not easy to compare this work with the previous work.<sup>14</sup> In the previous work, PLA/SBP composites (0–45% w/w SBP) were compression-molded at 200°C. In the work presented here, PLA/SBP composites were processed with three separate thermal or mechanical treatments (extrusion, pelletization, and injection molding). When quenching is performed below the glass-transition temperature ( $T_g$ ), the polymer chains are not in equilibrium and will, in time, relax toward equilibrium. This process is called *enthalpic relaxation*, and it is thermodynamically driven.<sup>15,16</sup> The occurrence of enthalpic relaxation phenomena causes changes in the mechanical properties of the polymer: the polymer becomes brittle with reduced elongation to break in a process called *physical aging*.<sup>17</sup> The aging process can be determined by the storage of the polymer below  $T_g$  for a specific period. The enthalpic relaxation is a process that is nonlinear with time. It describes the relaxation of a wide range of molecules that have different molecular weights and thus relax at different times. The objective of this research was to evaluate SBP as a low-cost filler for PLA to produce green polymer composites with mechanical properties suitable for lightweight construction materials or automotive interior panels. Because PLA becomes brittle when stored below  $T_g$ , this work focuses on determining the enthalpic relaxation of the composites. The enthalpic relaxation can predict the magnitude of the aging effect on the polymer.

## EXPERIMENTAL

### Materials

SBP, provided by Williamette Valley Co. (Eugene, OR), was ground and passed through a 300-mesh screen. The residual moisture of SBP was 13.4% (w/

w) before extrusion processing. The composition of SBP was approximately 75% carbohydrates (pectin, cellulose, and hemicellulose), 9% protein, 6% ash, 9% lignin, and less than 1% oil. Tree-Top Orchards (Selah, WA) provided apple pulp (solid residue from pressing apples in the manufacture of cider) from the 2004 harvest. The pulp was dried and ground to a particle diameter of less than 300  $\mu\text{m}$ . The apple pulp, with about 5% moisture, was approximately 40% cellulose, 30% pectin, 10% protein, and 10% lignin.

PLA, provided by Cargill Dow (Minneapolis, MN), contained over 90% L-lactide. The average molecular weight was 150,000. The  $T_g$  value and the melting temperature, determined by differential scanning calorimetry (DSC), were 61 and 151°C, respectively.

### Extrusion processing

Compounding was performed with a Werner-Pfleiderer ZSK30 corotating twin-screw extruder (Cope-ion Corp., Ramsey, NJ). The barrel was composed of 14 sections with a length/diameter ratio of 44 : 1. The screw configuration has been reported previously.<sup>18</sup> The screw speed was 130 rpm. PLA was fed into barrel section 1 with a gravimetric feeder (model 3000, AccuRate, Inc., Whitewater, WI). After the melting of PLA, SBP was fed into barrel section 7 with a loss-in-weight feeder. The barrel was heated with eight heating zones. The temperature profile was 135 (zone 1), 190 (zone 2), and 177°C (zones 3–8). A die plate with 2 holes (4 mm in diameter) was used for extrusion. The melt temperature of the exudates at the die was approximately 160°C. The residence time was approximately 2.5 min. The die pressure and torque were allowed to stabilize between the formulations before the sample was collected. Strands were pelletized with a 2-in. laboratory pelletizer (Killion Extruders, Inc., Cedar Grove, NJ).

### Injection-molding

An ACT75B injection molder (Cincinnati Milacron, Batavia, OH) was used to injection-mold ASTM D 638-99 type I tensile bars (Master Precision Mold, Greenville, MI).<sup>21</sup> The barrel temperature profiles had to be adjusted to help move the material forward through the cooling of the feed section. The cooling time was increased as the samples with high weight fractions of SBP did not extrude as well as neat PLA. The shot size had to be increased slightly as the material density decreased with increased pulp content. The packing pressures were inverted for PLA/SBP composites with over 15% SBP because of extreme flashing characteristics. Other conditions included a hot sprue bushing (D-M-E, Madison Heights, MI) temperature of 177°C and a maximum injection pressure of 12,000 psi.

## DSC

The samples were analyzed with a TA Instruments (New Castle, DE) modulated DSC Q1000 equipped with a refrigeration cooling system. The samples (50 mg) were loaded and sealed in high-volume stainless steel pans (TA Instruments). The samples were run at a 10°C/min ramp speed from 0 to 200°C, isothermed for 1 min, cooled at 10°C/min back to 0°C, and isothermed for 1 min. The DSC instrument was calibrated against an indium standard. A nitrogen flow rate of 24 cm<sup>3</sup>/min was maintained during the run to purge the DSC cell as specified by the manufacturer. The DSC parameters, such as the enthalpy ( $\Delta H$ ) and temperature values, were calculated with TA Instruments software, with which the onset, peak, and end temperatures of transition were determined, and the area under the curve was used as the  $\Delta H$  value. This method was developed in our laboratory after consultation with the PLA certificate of analysis provided by Cargill Dow. Because the PLA melting temperature (180°C) was higher than  $T_g$  of SBP (63°C), it was used as the upper limit of heating.

## Aging study

Neat PLA, EX and extruded/injection-molded (EXIM) PLA, and EX and EXIM PLA/SBP and PLA/apple composites (85:15 or 70:30 PLA/SBP) were prepared for an aging study after they were melted by heating in a DSC pan up to 200°C and quench-cooled by immersion in liquid nitrogen. After the melting and quench cooling, the samples were stored in the DSC pan until further analysis. The aging study was performed after 0, 7, 15, and 30 days of storage at room temperature. The extent of the aging process was measured by the magnitude of the enthalpic relaxation.

## Thermogravimetric analysis (TGA)

TGA measurements were taken with a TGA 2050 thermogravimetric analyzer (TA Instruments). The composites were ground into powder with a Brinkmann/Retsch high-speed shaker mill (New Castle, DE). The samples (~10 mg) were heated from room temperature to 800°C at 10°C/min and held at an isotherm for 3 min. The TGA data were plotted as the temperature versus the weight percentage, from which the onset and final decomposition temperatures were obtained. Hereafter, these plots are called TGA plots. The TGA data were also plotted as the temperature versus the derivative of the weight percentage, from which the peak decomposition temperatures were obtained.

TGA was also used to determine the degradation kinetics of neat PLA and its composites. Each sample

was heated at three different rates (10, 15, and 20°C/min) in two atmospheres (nitrogen and air). After the analysis, kinetic data were determined with TA Specialty Library software with the activation energies reported at 50% conversion. Three heating rates were used to calculate the activation energy of degradation ( $E_a$ ) with the Flynn and Walls equation:<sup>19</sup>

$$\log \beta \cong 0.457 \left( -\frac{E_a}{RT} \right) + \left[ \log \left( \frac{AE_a}{R} \right) - \log F(a) - 2.315 \right]$$

where  $\beta$  is the heating rate,  $T$  is the absolute temperature,  $R$  is the gas constant,  $a$  is the conversion,  $A$  is the pre-exponential factor, and  $F(a)$  is the integral function of conversion ( $a$ ). According to this equation, at the same conversion,  $E_a$  can be obtained from the slope of the plot of  $\log \beta$  versus  $1000/T$  (K).  $E_a$  was calculated with the software provided by TA Instruments. The  $E_a$  value was determined for all samples at each heating rate, and the conversion percentage per minute was reported.

## Enzymatic degradation

Samples of EXIM PLA/SBP or PLA/apple composites were cut to similar dimensions (10 mm  $\times$  10 mm  $\times$  3.5 mm).<sup>20</sup> For neat PLA and EX PLA/SBP samples, four pieces of each sample were used. An enzyme buffer (0.05M Tris-HCl, pH 8.6) was prepared (0.91 g of Tris dissolved in 150 mL of Millipore water and adjusted to 8.6 with 1N HCl). Proteinase K enzyme (60 mg containing 7.5 units/mg of solid) and 30 mg of sodium azide were added to 150 mL of the buffer. Each sample was immersed in 5 mL of the enzyme buffer and stored at 37°C with occasional shaking. After 24 h, the enzyme solution of each sample was replaced with fresh buffer to maintain the maximum enzymatic activity. After 72 h of storage, the samples were rinsed with distilled water and dried *in vacuo* for 24 h. The difference in the weights before and after the enzyme treatment was recorded, and the weight-loss percentage was calculated. Dried and enzyme-treated samples were mounted onto aluminum specimen holders with silver paint (Fullman, Inc., Latham, NY) and were coated *in vacuo* with gold and palladium at 200/min in a blank sputter coating unit. The samples were then observed and photographed with a scanning electron microscope (JXM 6400, JEOL, Ltd., Tokyo, Japan) at 10 kV.

## Statistics

A single-factor, mixed-model analysis of variance was used to examine the weight-loss differences (%) resulting from enzymatic degradation between composites for each extrusion treatment. The fiber ratios were used as replications in the analyses. If the com-

posite effect from an analysis of variance  $F$ -test statistic was significant at  $p \leq 0.05$ , differences of least-square means were used to determine which composites were different from the others. A determination was also made of whether any weight-loss estimate for a particular composite was significantly different from 0 for each extrusion treatment (i.e., if the weight loss was not significantly different from 0, then no weight loss occurred). All analyses were performed with PROC MIXED in SAS PC for Windows (version 9.1.3).

The DSC data for the composites were analyzed with multiple regressions. The experiment consisted of two PLA composites (PLA/SBP and PLA/apple), three fiber ratios [neat (0), 15, and 30], four ages (0, 7, 15, and 30 days), and 2 extrusion methods (EX and EXIM). Five dependent variables were examined: the middle  $T_g$ ,  $\Delta C_p$  for  $T_g$  (J/g/°C), the enthalpic relaxation of extrusion, the crystallization enthalpy (J/g), and the melting enthalpy (J/g). For each PLA composite, 40 regression equations of the dependent variables as a function of the fiber ratio were obtained (five dependent variables  $\times$  four ages  $\times$  two extrusion methods) for a total of 80 equations. The predicted values of the dependent variables were obtained to compare neat samples (0) and samples with fiber ratios of 15 and 30 for each composite, age, and extrusion method combination with 95% confidence intervals. If the confidence intervals for predicted values overlapped, then the values were not significantly different from one another. All analyses were performed with TableCurve 2D (version 5.00, AISN Software).

## RESULTS AND DISCUSSION

The DSC analysis provided information required for determining: (1)  $T_g$  and  $\Delta C_p$ , (2) the enthalpic relaxation, (3) the crystallization and melting temperatures and  $\Delta H$ , and (4) the crystallinity percentage. These parameters were measured at different storage times to determine the effect of the storage time on the composite because polymer composites tend to phase-separate with time. The  $T_g$  values of PLA and its composites were mutually affected by the process type (EX or EXIM) and the presence of fibers. The data were analyzed with multiple regression. Tables I–IV list the data analyzed for both fibers, including the fiber levels (0, 15, and 30%) and aging time (0, 7, 15, and 30 days) for both SBP and apple fibers. The presence of SBP lowered  $T_g$  of EX PLA significantly at all storage times (Table I). The  $\Delta C_p$  data for EX PLA showed mixed effects: at 0, 7, and 15 days, it was significantly reduced, and at 30 days, it remained unchanged. The reduction of  $\Delta C_p$  indicated that the presence of SBP created a less compact PLA

**TABLE I**  
Effects of the Sugar Beet Level and Storage on the Dependent Variables ( $T_g$ , Crystallization, and Melting Temperature) of EX PLA/Sugar Beet Blends According to Regression Analysis

0 days		
Sugar beet (%)	$T_g$ (°C)	$\Delta C_p$ (J/g/°C)
0	60.27 <i>a</i>	0.47 <i>a</i>
15	54.87 <i>b</i>	0.46 <i>a</i>
30	52.91 <i>c</i>	0.39 <i>b</i>
Sugar beet (%)	Crystallization enthalpy (J/g)	Melting enthalpy (J/g)
0	1.24 <i>c</i>	0.75 <i>c</i>
15	2.40 <i>b</i>	3.12 <i>b</i>
30	5.50 <i>a</i>	7.11 <i>a</i>
7 days		
Sugar beet (%)	$T_g$ (°C)	$\Delta C_p$ (J/g/°C)
0	59.09 <i>a</i>	0.54 <i>a</i>
15	56.48 <i>b</i>	0.51 <i>b</i>
30	55.43 <i>c</i>	0.48 <i>c</i>
Sugar beet (%)	Crystallization enthalpy (J/g)	Melting enthalpy (J/g)
0	1.22 <i>c</i>	0.58 <i>c</i>
15	2.54 <i>b</i>	2.87 <i>b</i>
30	6.21 <i>a</i>	7.98 <i>a</i>
15 days		
Sugar beet (%)	$T_g$ (°C)	$\Delta C_p$ (J/g/°C)
0	59.86 <i>a</i>	0.541 <i>a</i>
15	57.14 <i>b</i>	0.541 <i>a</i>
30	56.05 <i>b</i>	0.508 <i>b</i>
Sugar beet (%)	Crystallization enthalpy (J/g)	Melting enthalpy (J/g)
0	1.19 <i>c</i>	0.66 <i>c</i>
15	2.83 <i>b</i>	3.59 <i>b</i>
30	6.59 <i>a</i>	8.41 <i>a</i>
30 days		
Sugar beet (%)	$T_g$ (°C)	$\Delta C_p$ (J/g/°C)
0	60.38 <i>a</i>	0.545
15	58.05 <i>b</i>	0.545
30	57.12 <i>c</i>	0.500
Sugar beet (%)	Crystallization enthalpy (J/g)	Melting enthalpy (J/g)
0	1.21 <i>c</i>	0.669 <i>c</i>
15	2.73 <i>b</i>	3.824 <i>b</i>
30	6.18 <i>a</i>	7.872 <i>a</i>

The means within columns and storage days with no letters are not significantly different ( $a > b > c$ ).



in which the molecules required less energy to become mobile. The  $\Delta H$  values of crystallization and melting of EX PLA increased at all SBP levels and storage times (Table I). This indicated that the presence of SBP helped the PLA molecules to pack better and form bigger and more compact crystals. The EXIM PLA samples exhibited no significant affect on  $T_g$  or  $\Delta C_p$  at 0 and 7 days of storage, but it was reduced for the remaining storage times (Table II). As seen for the EX samples, the EXIM samples exhibited an increase in the  $\Delta H$  values of crystallization and melting.

The EX apple fiber blends displayed a trend indicative of less influence on the PLA thermal properties.  $T_g$  was significantly reduced only after 15 and 30 days of storage time (Table III).  $\Delta C_p$  was significantly reduced at all storage times. This indicates a reduction of the amount of amorphous PLA material in the presence of apple fibers after extrusion. Table III also shows that the crystallization and melting peaks were not influenced significantly by the extrusion and apple fibers. The EXIM apple blend exhibited a reduction in  $\Delta C_p$  at all storage times, with some exceptions. Tables I–IV show that the presence of SBP had more influence on some of PLA's thermal properties than the apple and the processing method. Injection molding was also found to have little influence in the presence of apple fibers.

The crystallinity percentage at this temperature was calculated by the subtraction of crystallization enthalpy and second crystallization enthalpy ( $\Delta H_c$  and  $\Delta H_{c2}$ ) from the enthalpy of fusion ( $\Delta H_f$ ) with the following equation:

$$\text{Crystallinity (\%)} = 100 \left( \frac{\Delta H_f - \Delta H_{c2}}{93.6} \right)$$

where 93.6 J/g is the reported  $\Delta H_f$  value for a PLA sample that was 100% crystalline.<sup>19</sup> The crystallinity percentage of unprocessed PLA dropped from 22.7 to 0.75 and 4.31% for EX and EXIM, respectively (Table V). This drop was due to the processing conditions during extrusion and injection molding, such as the shear, the temperature, and, most importantly, the temperature during cooling after processing. At 15% SBP, the composite exhibited 2.52% crystallinity for the EX sample and 9.63% for the EXIM sample, whereas the 30% SBP showed values of 4.44% and 11.46% for the EX and EXIM samples, respectively (Table V). This trend of the crystallinity percentage increasing in the presence of SBP was shown earlier to affect the  $\Delta H$  values of melting and the exothermic transition values. The crystallinity percentage remained unchanged as a function of the aging time; however, it increased through injection molding in the presence of SBP in the composite. The higher crystallinity was possibly due to slow cooling after

**TABLE II**  
Effects of the Sugar Beet Level and Storage on the Dependent Variables ( $T_g$ , Crystallization, and Melting Temperature) of EXIM PLA/Sugar Beet Blends According to Regression Analysis

0 days		
Sugar beet (%)	$T_g$ (°C)	$\Delta C_p$ (J/g/°C)
0	60.65	0.44
15	54.60	0.44
30	54.60	0.43
Sugar beet (%)	Crystallization enthalpy (J/g)	Melting enthalpy (J/g)
0	3.23 <i>b</i>	2.62 <i>b</i>
15	5.94 <i>ab</i>	7.02 <i>ab</i>
30	8.65 <i>a</i>	9.58 <i>a</i>
7 days		
Sugar beet (%)	$T_g$ (°C)	$\Delta C_p$ (J/g/°C)
0	58.45	0.54
15	55.65	0.54
30	55.65	0.48
Sugar beet (%)	Crystallization enthalpy (J/g)	Melting enthalpy (J/g)
0	3.134 <i>c</i>	2.70 <i>c</i>
15	5.967 <i>b</i>	6.82 <i>b</i>
30	8.799 <i>a</i>	10.01 <i>a</i>
15 days		
Sugar beet (%)	$T_g$ (°C)	$\Delta C_p$ (J/g/°C)
0	59.31 <i>a</i>	0.524 <i>c</i>
15	57.01 <i>b</i>	0.534 <i>b</i>
30	56.09 <i>b</i>	0.538 <i>a</i>
Sugar beet (%)	Crystallization enthalpy (J/g)	Melting enthalpy (J/g)
0	3.21 <i>c</i>	2.69 <i>c</i>
15	7.67 <i>b</i>	7.96 <i>b</i>
30	10.07 <i>a</i>	10.96 <i>a</i>
30 days		
Sugar beet (%)	$T_g$ (°C)	$\Delta C_p$ (J/g/°C)
0	60.08 <i>a</i>	0.556 <i>a</i>
15	57.88 <i>b</i>	0.553 <i>a</i>
30	56.96 <i>c</i>	0.546 <i>b</i>
Sugar beet (%)	Crystallization enthalpy (J/g)	Melting enthalpy (J/g)
0	3.30 <i>c</i>	2.67 <i>c</i>
15	7.42 <i>b</i>	8.46 <i>b</i>
30	11.55 <i>a</i>	11.81 <i>a</i>

The means within columns and storage days with no letters are not significantly different ( $a > b > c$ ).

**TABLE III**  
Effects of the Apple Fiber Level and Storage on the Dependent Variables ( $T_g$ , Crystallization, and Melting Temperature) of EX PLA/Apple Fiber Blends According to Regression Analysis

0 days		
Apple (%)	$T_g$ (°C)	$\Delta C_p$ (J/g/°C)
0	60.32	0.47 <i>a</i>
15	56.47	0.45 <i>b</i>
30	54.80	0.37 <i>c</i>
Apple (%)	Crystallization enthalpy (J/g)	Melting enthalpy (J/g)
0	1.22	0.65
15	21.94	22.56
30	17.86	18.28
7 days		
Apple (%)	$T_g$ (°C)	$\Delta C_p$ (J/g/°C)
0	59.10	0.53 <i>a</i>
15	57.36	0.48 <i>b</i>
30	57.34	0.42 <i>c</i>
Apple (%)	Crystallization enthalpy (J/g)	Melting enthalpy (J/g)
0	1.19	0.57
15	21.24	21.76
30	17.27	17.59
15 days		
Apple (%)	$T_g$ (°C)	$\Delta C_p$ (J/g/°C)
0	59.86 <i>a</i>	0.54 <i>a</i>
15	58.54 <i>b</i>	0.49 <i>b</i>
30	58.00 <i>c</i>	0.44 <i>c</i>
Apple (%)	Crystallization enthalpy (J/g)	Melting enthalpy (J/g)
0	1.20	0.66 <i>c</i>
15	21.58	21.27 <i>a</i>
30	17.55	17.25 <i>b</i>
30 days		
Apple (%)	$T_g$ (°C)	$\Delta C_p$ (J/g/°C)
0	60.5 <i>a</i>	0.53 <i>a</i>
15	59.30 <i>b</i>	0.51 <i>b</i>
30	58.40 <i>c</i>	0.45 <i>c</i>
Apple (%)	Crystallization enthalpy (J/g)	Melting enthalpy (J/g)
0	1.22	0.63
15	23.07	23.83
30	18.79	19.31

The means within columns and storage days with no letters are not significantly different at 95% confidence intervals ( $a > b > c$ ).

**TABLE IV**  
Effects of the Apple Fiber Level and Storage on the Dependent Variables ( $T_g$ , Crystallization, and Melting Temperature) of EXIM PLA/Apple Fiber Blends According to Regression Analysis

0 days		
Apple (%)	$T_g$ (°C)	$\Delta C_p$ (J/g/°C)
0	60.60 <i>a</i>	0.48
15	58.34 <i>b</i>	0.48
30	54.61 <i>c</i>	0.41
Apple (%)	Crystallization enthalpy (J/g)	Melting enthalpy (J/g)
0	3.51 <i>b</i>	2.63
15	23.10 <i>a</i>	25.02
30	23.10 <i>a</i>	25.03
7 days		
Apple (%)	$T_g$ (°C)	$\Delta C_p$ (J/g/°C)
0	58.48	0.53 <i>a</i>
15	56.40	0.51 <i>b</i>
30	55.52	0.43 <i>c</i>
Apple (%)	Crystallization enthalpy (J/g)	Melting enthalpy (J/g)
0	3.10	2.64 <i>b</i>
15	25.89	24.75 <i>a</i>
30	21.47	24.75 <i>a</i>
15 days		
Apple (%)	$T_g$ (°C)	$\Delta C_p$ (J/g/°C)
0	59.36	0.52 <i>a</i>
15	58.08	0.51 <i>b</i>
30	56.76	0.45 <i>c</i>
Apple (%)	Crystallization enthalpy (J/g)	Melting enthalpy (J/g)
0	3.23	2.59
15	25.17	26.38
30	20.91	21.79
30 days		
Apple (%)	$T_g$ (°C)	$\Delta C_p$ (J/g/°C)
0	60.1	0.55 <i>a</i>
15	58.60	0.52 <i>b</i>
30	58.60	0.45 <i>c</i>
Apple (%)	Crystallization enthalpy (J/g)	Melting enthalpy (J/g)
0	3.30	2.75
15	25.95	26.97
30	21.53	22.3

The means within columns and storage days with no letters are not significantly different at 95% confidence intervals ( $a > b > c$ ).

**TABLE V**  
**Values of  $E_a$  (in Air and Nitrogen), the Crystallinity (%), and the Weight Loss (%) After the Enzymatic Treatment of Neat PLA and PLA/Fiber (SBP and Apple) Composites**

Sample	PLA/fiber ratio <sup>a</sup>	Process	$E_a$ in air (J/g)	$E_a$ in N <sub>2</sub> (J/g)	Crystallinity (%)	Weight loss after the enzymatic treatment (%) <sup>d</sup>
Neat PLA	0	Unprocessed	143.0	218.3	22.7	7.0
EX PLA	0	EX	195.7	183.1	0.75	0.5
Molded PLA	0	Injection-molded	165.0	163.5	4.31	1.4
PLA/SBP	15	EX	270.7	61.5	2.52	4.4
PLA/SBP	15	Injection-molded	122.7	67.8	9.63	1.7
PLA/SBP	30	EX	239.8	16.5	4.44	10.0
PLA/SBP	30	Injection-molded	190.2	172.8	11.46	1.5
PLA/apple	15	EX	145.0	120.5	3.31	10.2
PLA/apple	15	Injection-molded	172.9	125.9	2.56	3.1
PLA/apple	30	EX	186.4	175.0	2.99	16.2
PLA/apple	30	Injection-molded	168.2	151.7	1.98	4.4

the injection-molding process and the orientation of PLA molecules or the formation of a continuous PLA phase. Injection molding oriented PLA and SBP along the direction of flow, that is, axially. The highest crystallinity was noted at 30% SBP for the EXIM sample (11%), and the lowest was recorded for the neat EX PLA sample (1.2%). Overall, apple fibers were less effective in changing the PLA crystallinity than SBP, but the EX apple fiber/PLA composite increased in its crystallinity fourfold.

The physical aging behavior of PLA was determined with the DSC data. Because the aging is closely related to the cooling rate, all samples were melted and quench-cooled by immersion in liquid nitrogen while in the pan. The melting and quench cooling reset the thermal history of the sample to zero, thereby erasing the previous thermal history. The aging process of PLA was monitored through the measurement of the enthalpic relaxation, which is an endothermic transition under the glass-transition profile (Fig. 1).<sup>20</sup> The enthalpic relaxation steadily

increased with the storage time at room temperature. Because the enthalpic relaxation was a time-dependent process, it had no value at a storage time of 0. The enthalpic relaxation of neat EX PLA increased significantly from 0 to 0.067 to 0.46 to 1.13 J/g after storage for 0, 7, 15, and 30 days, respectively (Fig. 2). Comparable trends were true for PLA/SBP and PLA/apple fiber composites. The EXIM samples showed higher enthalpic relaxation than the EX samples. That could be due to the cooling rate difference between the EX and EXIM samples (Fig. 2). Our data are somewhat different from those of the literature reports,<sup>20</sup> which showed that the enthalpic relaxation increased at a slower rate after 6 days of storage. Unlike the literature, the enthalpic relaxation of our samples increased steadily during the month of storage and showed no indication of leveling off. The differences could stem from the molecular properties of PLA and the processing conditions. The nature of the data collection, which involved the experimental design and instrument sensitivity, could also cause

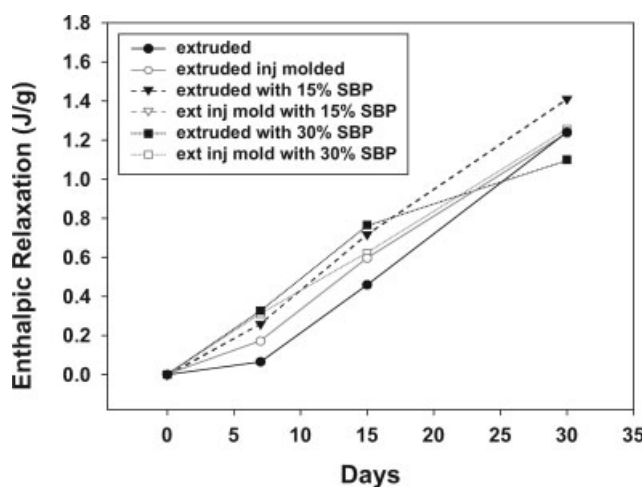


**Figure 1** Effect of aging on the enthalpic relaxation of EX and EXIM PLA/SBP composites.

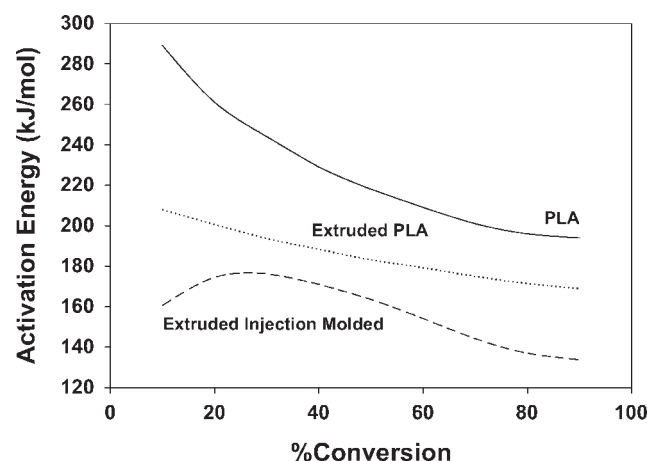


**Figure 2** TGA  $E_a$  values of unprocessed, EX, and EXIM neat PLA samples as a function of the conversion (%) in nitrogen.

**TABLE VI**  
**TGA Degradation of PLA Composites Listed as the Conversion (%) for All EX and EXIM Composites**  
**in Air and in Nitrogen**

PLA	Ratio <sup>c</sup>	Process	10% <sup>d</sup>	20%	30%	40%	50%	60%	70%	80%	90%
PLA <sup>a</sup>	0	As is	289.8	261.8	244.2	229.7	218.3	209.2	201.8	196.7	194.5
PLA <sup>a</sup>	0	Extruded	207.9	200.6	193.6	188.3	183.1	179.2	174.9	171.4	168.8
PLA <sup>a</sup>	0	Injection Molded	160.6	171.5	176.2	171.0	163.5	154.0	144.1	136.9	133.6
PLA:SBP <sup>a</sup>	85:15	Extruded	56.9	57.5	60.9	61.6	61.5	62.0	64.0	69.5	77.8
PLA:SBP <sup>a</sup>	85:15	Injection Molded	75.8	71.5	70.7	69.2	67.8	67.5	68.9	71.4	75.6
PLA:SBP <sup>a</sup>	70:30	Extruded	364.7	238.6	200.1	176.6	160.5	145.2	126.2	123.0	207.1
PLA:SBP <sup>a</sup>	70:30	Injection Molded	112.3	132.4	157.1	170.7	172.8	173.1	173.6	180.5	201.5
PLA:Apple <sup>a</sup>	85:15	Extruded	114.7	108.4	109.6	113.3	120.5	130.4	145.8	167.9	181.4
PLA:Apple <sup>a</sup>	85:15	Injection Molded	126.6	128.3	126.2	125.1	125.9	129.9	130.0	134.4	144.7
PLA:Apple <sup>a</sup>	70:30	Extruded	373.0	261.4	213.6	190.1	175.0	162.6	148.0	168.5	220.2
PLA:Apple <sup>a</sup>	70:30	Injection Molded	207.3	157.0	152.0	151.4	151.7	155.9	161.6	170.7	174.0
PLA <sup>b</sup>	0	As is	144.9	166.6	164.7	156.1	143.0	131.6	127.5	128.1	128.4
PLA <sup>b</sup>	0	Extruded	223.6	261.4	248.8	213.4	195.7	187.8	181.2	175.2	169.1
PLA <sup>b</sup>	0	Injection Molded	193.3	204.7	196.2	177.9	165.0	159.4	155.7	151.0	143.7
PLA:SBP <sup>b</sup>	85:15	Extruded	219.3	248.0	281.1	288.6	270.7	234.1	208.4	199.5	207.8
PLA:SBP <sup>b</sup>	85:15	Injection Molded	139.3	159.1	169.4	143.7	122.7	111.2	110.2	114.7	119.1
PLA:SBP <sup>b</sup>	70:30	Extruded	292.3	235.3	242.2	252.8	239.8	222.9	230.9	242.5	301.3
PLA:SBP <sup>b</sup>	70:30	Injection Molded	110.5	202.7	278.7	239.3	190.2	162.6	160.1	157.2	166.0
PLA:Apple <sup>b</sup>	85:15	Extruded	139.4	158.5	159.9	150.5	145.0	143.5	143.9	145.2	152.3
PLA:Apple <sup>b</sup>	85:15	Injection Molded	194.6	228.9	214.2	191.8	172.9	161.5	158.8	165.1	189.5
PLA:Apple <sup>b</sup>	70:30	Extruded	217.7	202.5	201.5	191.0	186.4	193.5	204.1	233.5	140.2
PLA:Apple <sup>b</sup>	70:30	Injection Molded	166.9	212.8	198.0	179.7	168.2	157.1	146.8	141.4	175.2

<sup>a</sup> TGA test in nitrogen.

<sup>b</sup> TGA test in air.

<sup>c</sup> PLA/fiber ratio.

<sup>d</sup> Degradation conversion (%) of PLA/SBP and PLA/apple composites.

some variations. The presence of SBP fibers in concentrations of 15 and 30% significantly increased the enthalpic relaxation within the same number of storage days. Apple fibers within the same storage time increased the enthalpic relaxation, but it was not statistically significant.

$E_a$ , as mentioned in a previous section, was determined with TGA in both air and nitrogen with a method based on different heating rates.<sup>19</sup> Neat PLA was much more resistant to degradation in nitrogen than air (Table V). Injection-molded neat PLA exhibited lower  $E_a$  values than EX samples. In the presence of SBP, the EX composite showed a higher  $E_a$  value in air (Table V). Overall,  $E_a$  in air was much higher than that in nitrogen in the presence of both fibers. This indicated slow oxidation of the composites during heating. The temperature–conversion data in Table VI were used to calculate the  $E_a$  values for each composite in air and nitrogen. The plot of  $E_a$  as a function of the degradation and conversion (%) was used as predictor of the degradation mechanism.<sup>20</sup>  $E_a$  as a function of the conversion percentage (Fig. 2 and Table VI) showed that the degradation of unprocessed and EX neat PLA in N<sub>2</sub> was a one-step process, as indicated by a relatively straight line, whereas the EXIM sample showed a two-step process (Fig. 3). In air,  $E_a$  of unprocessed PLA degrada-

tion showed a two-step process possibly due to the oxidation rate in air versus that in nitrogen. The presence of 15% SBP exhibited a one-step degradation in N<sub>2</sub> with little change in  $E_a$  through the different levels of conversions, whereas in air, two or more steps were present (Table VI). The 30% SBP samples showed a multistep degradation process in air and in nitrogen. Generally, the EX samples exhibited a two-step continuous decrease in  $E_a$  as the conversion percentage increased, whereas the EXIM samples showed three distinct steps of degradation, as indicated by lines going in three different directions for the same sample (Table VI).

The enzymatic degradation of PLA was affected by the morphology of the material and thus the fiber content. The EXIM sample was covered with a film of PLA and fibers and was mostly accessible only from the cut edges (Fig. 4). The SEM data showed big differences between the surfaces of the unprocessed and injection-molded PLA samples. All samples were enzyme-treated, but from Figure 4, it is clear how processing could affect the final product of the enzymatic degradation rate. This information needs to be considered when biodegradation studies are carried out. In the EX composites, PLA and fibers were exposed and accessible to the enzyme for the most part. The weight loss after the proteinase



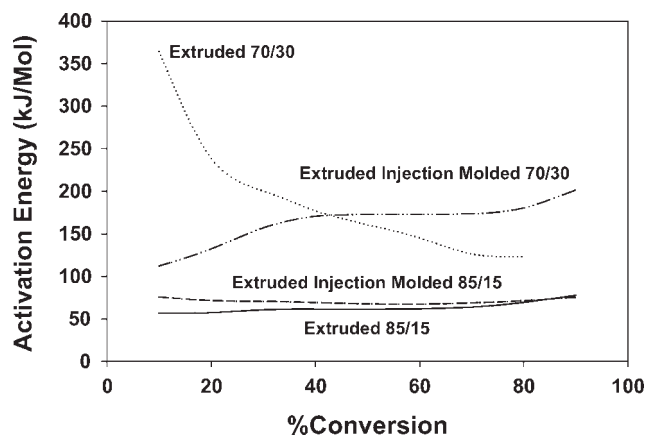


**Figure 3** TGA  $E_a$  values of EX and EXIM PLA/SBP samples (70 : 30 and 85 : 15) as a function of the conversion (%) in nitrogen.

treatment was very similar for the EXIM samples, regardless of whether neat PLA or a composite was used, except for the PLA/apple composite, for which the weight loss was twice as much (Table V). There were significant differences between the weight losses of the composites for both the EX and EXIM treatments ( $p = 0.0147$  and  $p = 0.009$ , respectively). Both treatments showed that the PLA/apple composites had significantly higher weight loss than SBP. In the EX and enzyme-treated samples, the PLA/apple sample had a significant weight loss ( $p = 0.0346$ ). In the EX and EXIM treatments, both the PLA/apple

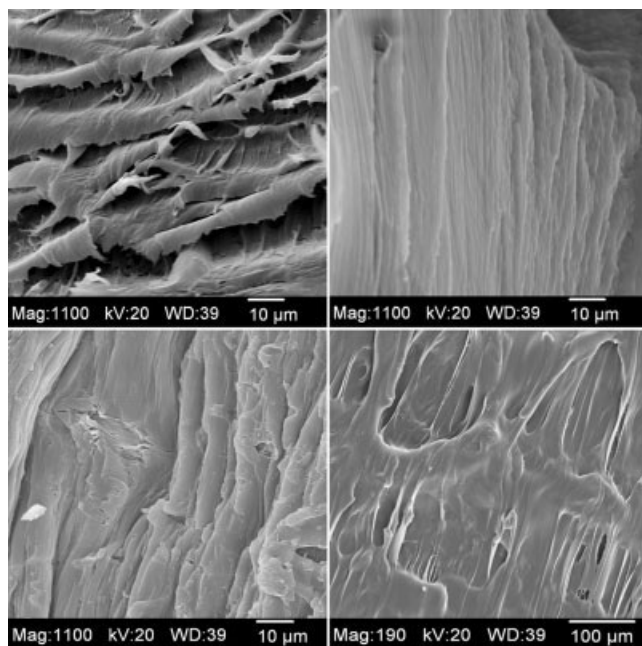


**Figure 4** Scanning electron micrographs of enzymatically treated neat PLA and PLA/SBP composites: (A) unprocessed neat PLA, (B) injection-molded neat PLA, (C) EX 70 : 30 PLA/SBP, and (D) EXIM 70 : 30 PLA/SBP.

and PLA/SBP composites showed significant weight losses ( $p = 0.0033$  and  $p = 0.0286$ , respectively). These data were consistent with the previously mentioned statement regarding the presence of higher crystallinity in the EXIM samples. The crystallinity percentage was plotted against the weight-loss percentage after the enzyme treatment, and this showed a relationship between the degree of crystallinity and enzyme accessibility (Fig. 5). The weight loss of the EX samples continued to increase with small changes in the crystallinity, whereas the EXIM weight loss remained unchanged with a sharp increase in the crystallinity (Fig. 5).

$T_g$ 's from DSC can be used to obtain qualitative and quantitative information about the properties of polymer mixtures. The properties and intermolecular force parameters that affect the miscibility of polymers can be correlated on the basis of DSC measurements.<sup>21–23</sup> These also include estimates of the degree of intermolecular interactions between mixture components. Generally, the miscibility of polymers can be measured by the presence of a single  $T_g$  or a shift in  $T_g$ .<sup>24</sup> Model equations, such as the Gordon–Taylor equation,<sup>25</sup> have been proposed to predict the  $T_g$  dependence of polymer composites from experimental data. The Gordon–Taylor equation for blends of PLA/fiber composites can be represented as follows:

$$T_g^b = \frac{W_1 T_{g1} + K W_2 T_{g2}}{W_1 + K W_2} \quad (1)$$

where  $T_g^b$  is the blend glass-transition temperature;  $W_1$  and  $W_2$  are the weight fractions of the sugar beet and PLA, respectively;  $T_{g1}$  and  $T_{g2}$  are the glass-transition temperatures of SBP and PLA, respectively; and  $K$  is an adjustable fitting parameter related to

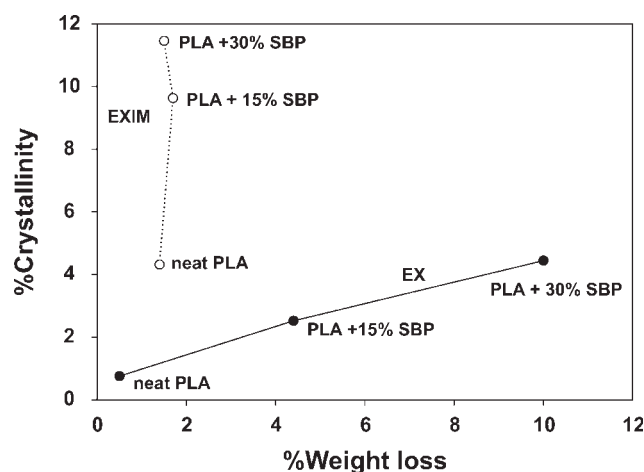


**Figure 5** Effect of the crystallinity (%) on the weight loss of neat PLA and PLA/SBP composites after an enzymatic treatment.

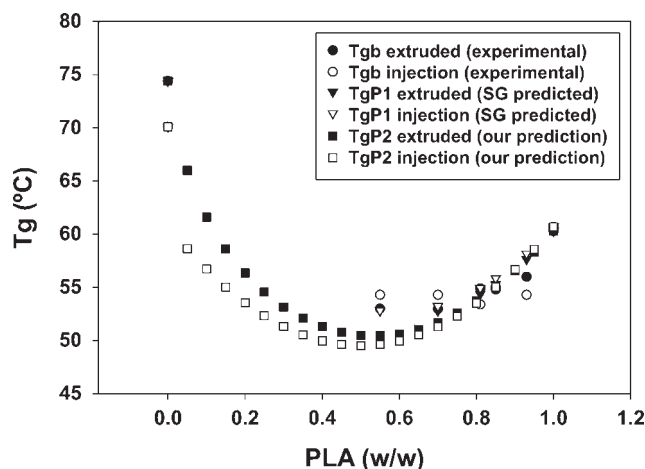


**Figure 6**  $T_g$  versus the composition in PLA/SBP composites. The  $T_g$  values were predicted with the Gordon–Taylor–Kwei equation with the  $K$  and  $q$  values listed in Table VII. Unlike the Gordon–Taylor–Wood equation, in which one  $T_g$  value is fixed, the Kwei method uses both  $T_g$  values for the best fit.

the miscibility, that is, the strength of the interaction between the two components. The value of  $K$  in eq. (1) is unique for different blend ratios.

For blends of PLA/fiber composites, the Gordon–Taylor equation can be used in the following form:

$$T_g^b = \frac{W_1 T_{g1} + K(1 - W_1) T_{g2}}{W_1 + K(1 - W_1)} \quad (2)$$

where  $W_1 = (1 - W_2)$  is the weight fraction of the sugar beets in the blend.

To estimate the degree of intermolecular interactions between mixture components, the Gordon–Taylor eq. (2) was modified by Kwei et al.<sup>26</sup> as follows:

$$T_g^b = \frac{W_1 T_{g1} + K(1 - W_1) T_{g2}}{W_1 + K(1 - W_1)} + q W_1 (1 - W_1) \quad (3)$$

where the parameter  $q$ , the coefficient of the interaction term, is regarded as a measure of the intermolecular interaction between components  $W_1$  and  $W_2$  when  $W_2 = (1 - W_1)$ . Both  $K$  and  $q$  are used to fit eq. (3) to experimental DSC data. The sign (positive or negative) of the value of the fitted parameter  $q$  indi-

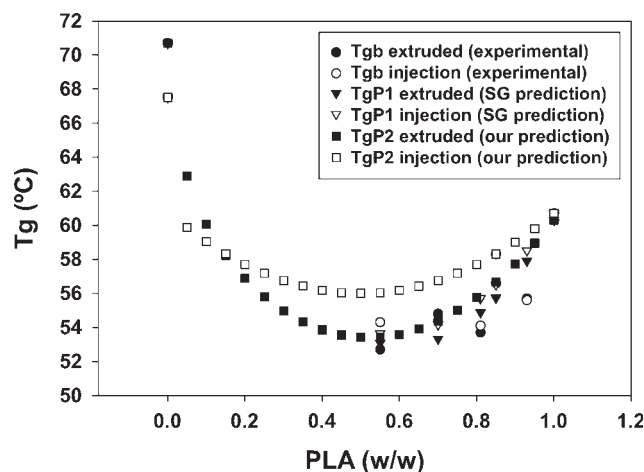


**Figure 7**  $T_g$  versus the composition in PLA/apple composites. The  $T_g$  values were predicted with the Gordon–Taylor–Kwei equation with the  $K$  and  $q$  values listed in Table VII. Unlike the Gordon–Taylor–Wood equation, in which one  $T_g$  value is fixed, the Kwei method uses both  $T_g$  values for the best fit.

cates the direction of the net change (increase or decrease) in the weight average of  $T_{g1}$  and  $T_{g2}$  produced by the interaction. The magnitude of the fitted parameter  $q$  indicates the strength of the net effect on  $T_g^b$  due to the various modes of intermolecular interactions.<sup>26</sup>

The Kwei modification [eq. (3)] was fitted to  $T_g^b$  for the four blends studied in this work. Seven data points were plotted with  $T_g^b$  values from five blend ratios and with the  $T_g$  values of the two neat polymers,  $T_{g1}$  and  $T_{g2}$ , as experimental DSC data. All results were similar to the sugar beet example shown in Figure 6. The computed  $K$  and  $q$  values are listed in Table VII with the correlation coefficients of the best fit for each blend.

The results in Table VII indicate that the best fit (correlation coefficient = 0.990497) with eq. (3) was obtained for a PLA/SBP composite (EX) blend, which gave  $K = 1.00130$  and  $q = -55.8837$ . In comparison with the other three blends, this showed the largest value of  $q$ , which indicated that the intermolecular interaction was strongest between the SBP and PLA EX materials. The results indicate that the intermolecular interaction was not as strong ( $q = -49.0289$ ) in the SBP/PLA EXIM sample. Although their  $q$  values were both significantly lower than those of the SBP/PLA samples, this greater effect of extrusion over injection molding on intermolecular interactions was also seen in the EX apple/PLA and EXIM apple/PLA samples (Fig. 7). The negative signs of the  $q$  values indicate that the intermolecular interaction was strong enough to drive the  $T_g$  values of the blends to  $T_g^b$  values below the  $T_{g1}$  and  $T_{g2}$  values of the neat polymers in all samples.<sup>15</sup>

**TABLE VII**  
Computed  $K$  and  $q$  Values from  $T_g^b$  Data with the Best Fit Correlation Coefficients

Blend	$K$	$q$	$R^2$
Sugar-PLA (extruded)	1.00130	-55.8837	0.990497
Sugar-PLA (injection)	0.99995	-49.0289	0.903572
Apple-PLA (extruded)	1.00012	-48.0598	0.959632
Apple-PLA (injection)	1.00012	-40.8767	0.898488

## CONCLUSIONS

Thermomechanical processing (EX and EXIM) has been found to affect the aging process of green polymer composites. The enthalpic relaxation showed a steady increase with aging. Injection molding increased the crystallinity percentage of neat PLA as well as its composites before aging. The degree of crystallinity remained the same for PLA through the aging period, whereas the presence of SBP and injection molding increased the crystallinity percentage of the composites. EX and EXIM created homogeneous composites. As the SBP polymer content increased, the degree of crystallinity increased. As the PLA and PLA/SBP composites aged, the PLA molecules relaxed, as shown by the enthalpic relaxation increasing.  $E_a$  indicated more than one step for the degradation mechanism. The enzymatic degradation rate was reduced by injection molding more than by composite composition.

The authors thank J. Adkins for conducting the modulated differential scanning calorimetry and thermogravimetric analysis experiments. The authors are also grateful for the contributions of Rick Haig, Brian Jasberg, Gary Grose, and Kathy Hornback to this work

## References

1. Netravali, A. N.; Chabba, S. *Mater Today* 2003, 6, 22.
2. Rothen-Weinhold, A.; Besseghir, K.; Vuaridel, E.; Sublet, E.; Oudry, N.; Kubel, F.; Gurny, R. *Eur J Pharm Biopharm* 1999, 48, 113.
3. Fang, Q.; Hanna, M. A. *Ind Crops Prod* 1999, 10, 47.
4. Nishino, T.; Hirao, K.; Kotera, M.; Nakamae, K.; Inagaki, H. *Compos Sci Technol* 2003, 63, 1281.
5. Oksman, K.; Skrifvars, M.; Selin, J. F. *Compos Sci Technol* 2003, 63, 1317.
6. Wollerdorfer, M.; Bader, H. *Ind Crops Prod* 1998, 8, 105.
7. Chen, C. C.; Chueh, J. Y.; Tseng, H.; Huang, H. M.; Lee, S. Y. *Biomaterials* 2003, 24, 1167.
8. Wang, L.; Ma, W.; Gross, R. A.; McCarthy, S. P. *Polym Degrad Stab* 1998, 59, 161.
9. Gattin, R.; Copinet, A.; Bertrand, C.; Couturier, Y. *Int Biodeterioration Biodegrad* 2002, 50, 25.
10. Martin, O.; Averous, L. *Polymer* 2001, 42, 6209.
11. Garlotta, D.; Doane, W. M.; Shogren, R. L.; Lawton, J. W.; Willett, J. L. *J Appl Polym Sci* 2003, 88, 1775.
12. Kasuga, T.; Maeda, H.; Kato, K.; Nogami, M.; Hata Ki, Ueda, M. *Biomaterials* 2003, 24, 3247.
13. Bleach, N. C.; Nazhat, S. N.; Tanner, K. E.; Kellomaki, M.; Tormala, P. *Biomaterials* 2002, 23, 1579.
14. Liu, L.; Onwulata, C.; Fishman, M. L.; Savary, B.; Hicks, K. B. *US Jpn Cooperative Res Nat Resour* 2004, 80.
15. Cao, X.; Mohamed, A.; Gordon, S. H.; Willett, J. L.; Sessa, D. J. *Thermochim Acta* 2003, 406, 115.
16. Nicolais, L.; Narkis, M. *J Appl Polym Sci* 1971, 15, 469.
17. Bailey, N. A.; Sandor, M.; Kreitz, M.; Mathiowitz, E. *J Appl Polym Sci* 2002, 86, 1868.
18. Finkenstadt, V. L.; Liu, L. S.; Willett, J. L. *J Polym Environ* 2007, 15, 1.
19. Flynn, J. H.; Wall, L. A. *Polym Lett* 1966, 323.
20. Hua, C.; Vipul, D.; Gross, R. A.; McCarthy, S. P. *J Polym Sci* 1996, 34, 2701.
21. *Structure-Property Relations in Polymers: Spectroscopy and Performance*; Urban, M. W.; Craver, C. D., Eds.; American Chemical Society: Washington, DC, 1993.
22. Liu, L. S.; Finkenstadt, V. L.; Liu, C. K.; Coffin, D. R.; Willett, J. L.; Fishman, M. L.; Hicks, K. B. *J Biobased Mater Bioenergy*, to appear.
23. Wong, A.C.-Y.; Lam, F. *Polym Test* 2002, 21, 691.
24. Urzua, M.; Gargallo, L.; Radic, D. *J Macromol Sci Phys* 2000, 39, 143.
25. Gordon, M.; Taylor, J. S. *J Appl Chem* 1952, 2, 493.
26. Kwei, T. K.; Pearce, E. M.; Pennacchia, J. R.; Charton, M. *Macromolecules* 1987, 20, 1174.